The isotope effect on impurities and bulk ion particle transport in the Large Helical Device

Isotope effect on impurity and bulk ion particle transport in the Large Helical Device

K. Ida,[1,2] R. Sakamoto,[1,2] M. Yoshinuma,[1,2] K. Yamazaki,[3] T. Kobayashi,[1,2] Y. Fujiwara,[1] C. Suzuki,[1] K. Fuji,[4] J. Chen,[5] I. Murakami,[1,2] M. Emoto,[1] R. Mackenbach,[6] H. Yamada,[1,2] G. Motojima,[1] S. Masuzaki,[1,2] K. Mukai,[1,2] K. Nagaoka,[1,7] H. Takahashi,[1,2] T. Oishi,[1,2] M. Goto,[1,2] S. Morita,[1,2] N. Tamura,[1,2] H. Nakano,[1,2] S. Kamio,[1] R. Seki,[1,2] M. Yokoyama,[1,2] S. Murakami,[8] M. Nunami,[1,2] M. Nakata,[1,2] T. Morisaki,[1,2] M. Osakabe,[1,2] and the LHD Experiment Group[1]

[1]*National Institute for Fusion Science, National Institutes of Natural Sciences, Toki, Gifu 509-5292, Japan*
[2]*SOKENDAI (The Graduate University for Advanced Studies), Toki, Gifu 509-5292, Japan*
[3]*Research Institute for Applied Mechanics Kyushu University, Kasuga, Fukuoka, Japan*
[4]*Department of Mechanical Engineering and Science, Graduate School of Engineering, Kyoto Univ., Kyoto 615-8540, Japan*
[5]*School of Nuclear Science and Technology, University of Science and Technology of China, Hefei 230026, China*
[6]*Eindhoven University of Technology Merovingersweg 1, 5616 JA Eindhoven, Netherland*
[7]*Division of Particle and Astrophysical Science, Graduate School of Science, Nagoya University, Nagoya, Aichi 464-8601, Japan*
[8]*Department of Nuclear Engineering, Kyoto University, Kyoto, Kyoto 615-8510, Japan*

(Dated: February 19, 2019)

Isotope effect on impurity and bulk ion particle transport is investigated by using the deuterium, hydrogen, and isotope mixture plasma in the Large Helical Device (LHD). A clear isotope effect is observed in the impurity transport but not the bulk ion transport. The isotope effects on impurity transport and ion heat transport are observed as a primary and a secondary effect, respectively, in the plasma with an internal transport barrier (ITB). In LHD, ion ITB is always transient because the impurity hole triggered by the increase of ion temperature gradient causes the enhancement of ion heat transport and gradually terminates the ion ITB. The formation of impurity hole becomes slower in the deuterium (D) plasma than the hydrogen (H) plasma. This primary isotope effect on impurity transport contributes the longer sustainment of ion ITB state because the low ion thermal diffusivity can be sustained as long as the normalized carbon impurity gradient $R/L_{n,c}$, where $L_c = -(\nabla n_c/n_c)^{-1}$, is above the critical value ($\sim$ -5). Therefore, the longer sustainment of ITB state in the deuterium plasma is considered to be a secondary isotope effect due to the mitigation of impurity hole. The radial profile of hydrogen (H) and deuterium (D) ion density is measured using bulk charge exchange spectroscopy inside the isotope mixture plasma. The decay time of H ion density after the H-pellet injection and the decay time of D ion density after D-pellet injection are almost identical, which demonstrates that there is no significant isotope effect on ion particle transport.

PACS numbers:

I. INTRODUCTION

Isotope effect on energy confinement and heat transport has been studied in toroidal devices and better confinement in the deuterium plasma is widely observed in several tokamaks. However, better confinement in the deuterium plasma is contrasted to the simple prediction from gyro-Bohm transport. This discrepancy implies that the mechanism of the better confinement in the deuterium plasma is much more complicated than the gyro-Bohm scaling and is not determined by the heat transport alone. The importance of the coupling among the heat, momentum, and particle, in particular, impurity particle transport, has been recognized to be important. This is because the turbulence level and heat transport depend on the plasma rotation, impurity density gradient as well as on the radial electric field shear. The impact of impurity density gradient on the instability and heat transport is one of the key issues in determining the level of heat transport, especially in the ion energy transport [1, 2].

In the one-species plasma, the transport of ion is degenerated due to the quasi-charge neutrality and ion density profile becomes identical to the electron profile regardless of the native ion transport. Depending on the type of instability, either an ion or electron transport determines the radial profile of electron and ion density. For example, when the ion temperature gradient (ITG) mode is dominant, the ion particle transport determines the radial profile of plasma density. In contrast, the electron particle transport determines the radial profile of plasma density when the electron temperature gradient (ETG) mode is dominant. In helical plasma, the non-ambipolar radial flux of ion and of electron are not equal in the condition of zero radial electric field. At the low-collisionality, the non-ambipolar radial flux of electrons is larger than that of ions and the radial electric field becomes positive. In contrast, the non-ambipolar radial flux of ion is larger than that of electron, and the radial electric field becomes negative [3]. The radial electric

field predicted by neoclassical theory in the plasma with high ion temperature is negative and convection velocity is expected to be inward. However, the convection velocity experimentally determined is outward [4]. Therefore, the turbulent transport is more dominant than the neoclassical transport in this experiment. In the isotope mixture plasma, each isotope can have a different profile, if the ion transport has strong isotope dependence, especially when the electron particle transport is dominant, because only the sum of the density of isotope species should be balanced to the electron to satisfy the quasi-charge neutrality condition. Therefore the isotope effect on ion particle (no electron transport) should be investigated in the isotope mixture plasma. It should be pointed out that the transport study in the D-H mixture plasma is essential in order to resolve the degeneration between ion particle transport and electron particle transport due to the quasi-neutralization condition.

In order to investigate the isotope effect on impurity and bulk ions, two experiments are performed in the heliotron-type Large Helical Device (LHD). One is the carbon pellet injection[5] into the hydrogen and deuterium plasma with internal transport barrier (ITB)[6] and the other is the hydrogen (H) and deuterium (D) pellet injection[7] into the D-H mixture plasma. It should be pointed out that the transport study in the D-H mixture plasma is essential in order to resolve degeneration between ion particle transport and electron particle transport due to the quasi-neutralization condition. In the case of impurity transport, impurity transport is always independent from electron transport because the electrons provided by impurities are negligibly small. Radial profiles of carbon impurity density and bulk ion density (fraction of H and D ion density) are measured using bulk charge exchange spectroscopy. In this paper, the isotope effect on impurity and its secondary effect on heat transport based on the carbon pellet injection experiment is described. The hydrogen and deuterium density profile measurements and the isotope effect of recycling on the particle ion transport after the pellet injection is also discussed.

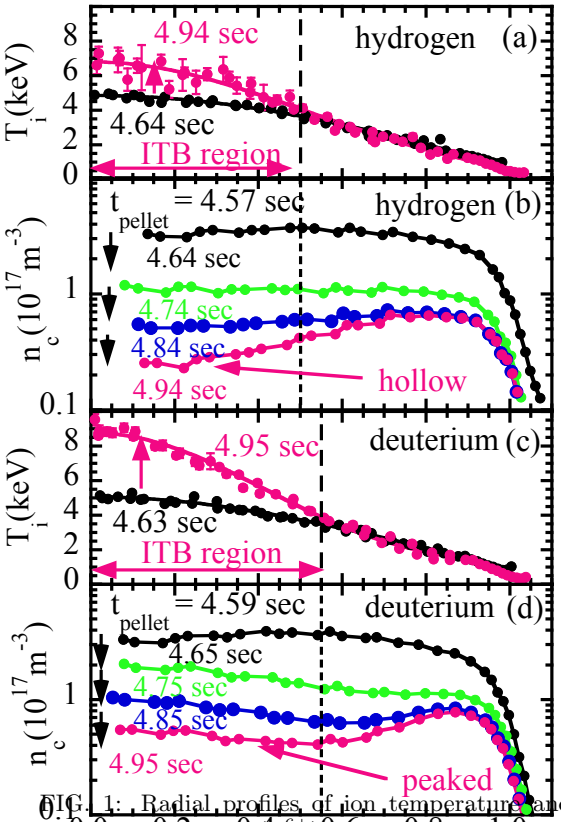

FIG. 1: Radial profiles of ion temperature and density of fully ionized carbon (C^{6+}) after the carbon pellet injection in the hydrogen (#123130) and deuterium (#133707) plasmas. The carbon density gradient is positive in the hydrogen ITB plasma, while it is negative in the deuterium ITB plasma.

II. ISOTOPE EFFECT ON IMPURITY AND HEAT TRANSPORT

There are various approaches to achieve the high performance plasma with an internal transport barrier (ITB)[8]. In LHD, the carbon pellet injection was found to be most effective to achieve the plasma with ITB, because it contributes to the decrease of electron temperature ion temperature ratio (T_e/T_i ratio) to unity[9], which is expected to stabilize the turbulence in the plasma and transient increase of effective heating power to accelerate slowing down process of beam ions in the low density plasma. The increase of carbon impurity does not cause the severe dilution problem, because of the strong impurity exhaust of the outward convection of impurity transport triggered by large ion temperature gradient. The increase of carbon impurity contributes the reduction of ion thermal diffusivity and the achievement of ITB[10]. However, achievement of ITB state by carbon pellet injection is transient due to the formation of impurity hole[4, 11, 12].

The carbon pellet injection is applied to trigger the formation of ion-ITB in the plasma with the magnetic axis of 3.6m, magnetic field strength of 2.85T, NBI power of $\sim$ 30 MW, and line averaged electron density of $1\times 10^{19}\mathrm{m}^{-3}$. During the decay phase of carbon density after the carbon pellet injection, the ion temperature (T_i) starts to increase from 5 keV to 7-9 keV, while the carbon density decreases by one order of magnitude. Differences in ion temperature profiles in Fig.1 (a) and (c) show the radial profile of ion temperature of fully ionized carbon (C^{6+}) measured with impurity charge exchange spectroscopy[13] in the plasma with ion -ITB in the hy-

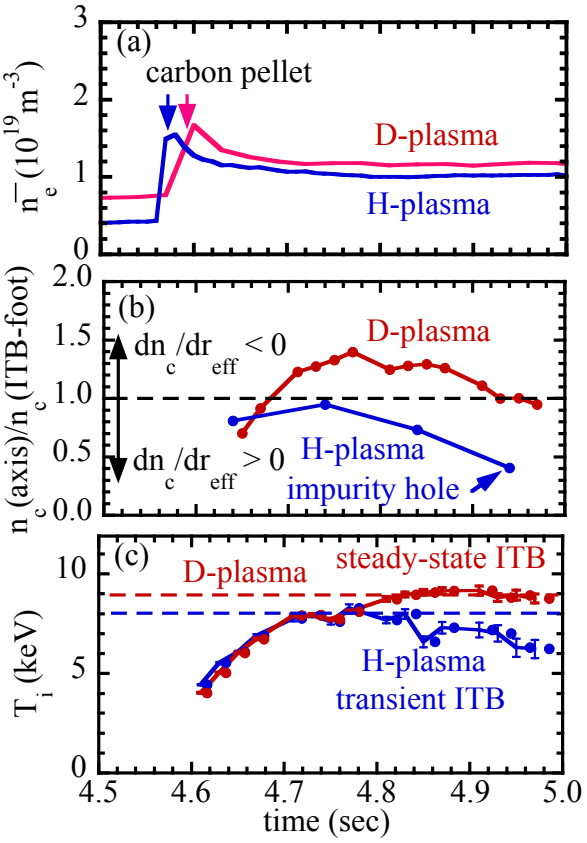

FIG. 2: Time evolution of (a) line-averaged electron density, (b) ratio of central carbon density to the carbon density at ITB-foot and (c) central ion temperature.

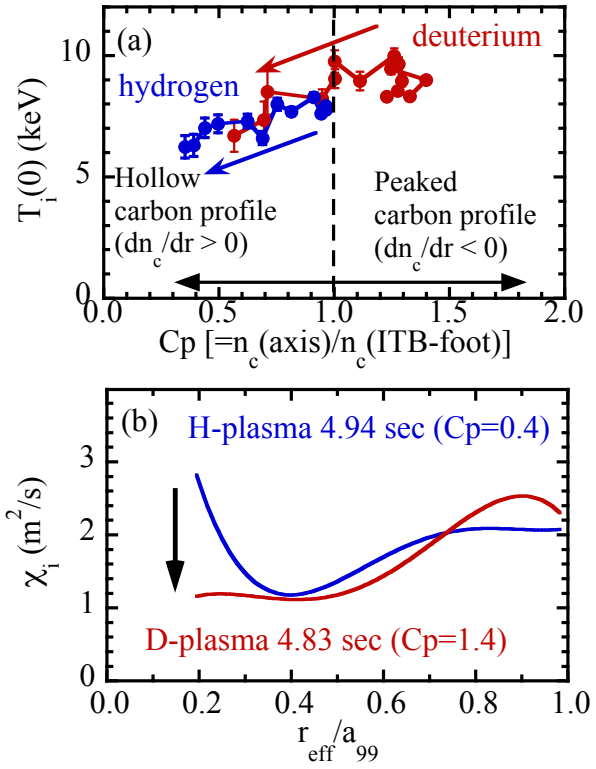

FIG. 3: (a) Central ion temperature as a function of the ratio of central carbon density to the carbon density at the ITB-foot (Cp) and (b) radial profile of ion thermal diffusivity in the deuterium (D) plasma with peaked carbon density profile (Cp = 1.4) and hydrogen (H) plasma with hollow carbon density profile ($Cp = 0.4$). Ion temperature starts to decrease due to the degradation of confinement after the carbon density peaking ratio, Cp, decrease below unity (positive gradient).

drogen and deuterium plasma. Fig.1 (b) and (d) show the radial profile of carbon density evaluated from the intensity of the carbon line measured with charge exchange spectroscopy combined with the beam attenuation calculation. The improvement of confinement (the increase of the ion temperature gradient) is observed within a certain radius, which is called as an ITB-foot location. Here ITB-region is defined as the region between the magnetic axis to ITB-foot location. Because the density profile is flat, turbulence measurements by Doppler reflectometer are now available. The phase contrast imaging (PCI) provides some information regarding turbulent fluctuation. Only the turbulent fluctuation near the ITB foot and not inside the ITB region can be measured with PCI. The wave number of the turbulent fluctuation is 0.2 mm^{-1} with the phase velocity of $1 \sim 4$ km/s in the ion diamagnetic direction at $r_{\rm eff}/a_{99} = 0.5$ [14].

The isotope effect is observed in the carbon density gradient inside the ITB region ($r_{\rm eff}/a_{99} < 0.55$ - 0.65). The carbon density gradient is positive in the H-plasma, while it is negative in the D-plasma. However, there is not any difference in the electron density profiles between H and D-plasmas. The carbon density profile just after the pellet injection is flat for both H and D-plasmas. However, the carbon density profile becomes hollow inside the ITB region in H-plasma, while the carbon density profile becomes peaked inside the ITB region of the D-plasmas. This behavior indicates the difference in convection velocity of impurity transport between H and D-plasmas due to the friction force between impurity and bulk ions. Recent ITG turbulence simulation reveals the isotope effects on impurity transport. It is predicted that convection velocity is significantly reduced by isotope effects, while isotope effects on diffusivity are relatively weak[15]. Mitigation of impurity hole experimentally observed in the deuterium plasma in LHD is also consistent with the prediction of the ITG turbulence simulation where the outward convection of light impurities is reduced in the deuterium plasma due to the isotope effects. It should be pointed out that the absolute carbon

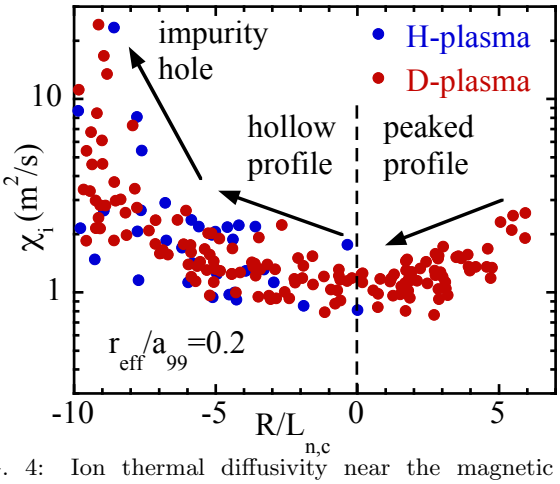

FIG. 4: Ion thermal diffusivity near the magnetic axis ($r_{\rm eff}/a_{99}$) as a function of normalized carbon density gradient of $R/L_{n,c}$ for hydrogen (H) and deuterium (D) plasma.

density is even lower in the deuterium plasma because of the smaller size of the carbon pellet injected. Although the fraction of the fully ionized carbon density (C^{6+}) is 3% of electron density immediately after the carbon pellet injection, the central fraction decreases sharply due to the formation of impurity hole and drops to the lower level of 0.3 $\sim$ 0.5% when the ion temperature reaches maximum value. Therefore, this result shows that the carbon density gradient (not the carbon density concentration) is an important parameter for the achievement of higher ion temperature. The sustainment of ITB state in the deuterium plasma is longer than that in the hydrogen plasma in LHD. Therefore, the achieved ion temperature is comparable just after the formation of ITB. However, the ion temperature in the deuterium plasma becomes higher than in the hydrogen plasma later phase of ITB state[16, 17].

Figure 2 displays the time evolution of electron density, the ratio of central carbon density to the carbon density at ITB- foot, and central ion temperature. The carbon pellet is injected at $t = 4.56$ sec. The line-averaged electron density increases sharply after the pellet injection and gradually decreases afterwards. In the hydrogen plasma, the central ion temperature starts to decrease after t = 4.74 sec due to the degradation of confinement after the carbon density ratio decreases to below unity (positive carbon density gradient). The carbon density ratio decreases to 0.5, which shows the formation of impurity hole characterized by the hollow impurity density profile. In contrast, carbon density ratio stays above unity (negative carbon density gradient) owing to the mitigation of impurity hole and there is no decrease of central ion temperature observed in the deuterium plasma. The longer sustainment of ion-ITB state in deuterium plasma is due to the mitigation of impurity hole formation (postponement of the appearance of positive impurity gradient). Even in the deuterium ITB plasma, the impurity hole appears and central ion temperature gradually decreases later in the discharge. The slow formation of impurity hole is due to the smaller diffusion coefficient and convection velocity in the deuterium plasma. The reduction of outward convection of impurity transport in deuterium plasma is the primary isotope effect and the longer sustainment of ITB state in the deuterium plasma is considered to be a secondary isotope effect due to the mitigation of impurity hollow.

Figure 3(a) shows the relation between the central ion temperature as an indicator of improvement of heat transport and the ratio of central carbon density to the carbon density at the ITB-foot. In both hydrogen and deuterium plasmas, the central ion temperature increases as the density ratio increased (density profile is peaked). No clear difference between hydrogen and deuterium plasma at the given carbon density gradient is observed. The correlation between the central ion temperature and the gradient of carbon density in the ITB region suggests that the positive carbon density (hollow carbon density profile) enhances the ion transport and prevents the steady-state sustainment of ion-ITB, where the impurity formation occurs due to the increase of the ion temperature gradient. Figure 3(b) shows the radial profile of ion thermal diffusivity in the deuterium (D) plasma with peaked carbon density profile ($Cp = 1.4$) and hydrogen (H) plasma with hollow carbon density profile ($Cp = 0.4$). The ion heat diffusivity in the outer region in the plasma ($r_{\rm eff}/a_{99} > 0.4$) is almost identical between hydrogen and deuterium plasma. The clear difference is observed in the core region ($r_{\rm eff}/a_{99} < 0.4$) inside ITB. The ion thermal diffusivity shows sharp increase towards the plasma center in the core region of the hydrogen plasma, while it is relatively flat in the deuterium plasma. Ion temperature begins to decrease due to the degradation of confinement (increase of core ion thermal diffusivity) after the carbon density peaking ratio, Cp, decreases to below unity (positive gradient).

Figure 4 shows the ion thermal diffusivity near the magnetic axis ($r_{\rm eff}/a_{99}$) as a function of normalized carbon density gradient of $R/L_{n,c}$ for hydrogen (H) and deuterium (D) plasma. Here the R is major radius and L_c is carbon density scale length defined as $L_{n,c} = -(\nabla n_c/n_c)^{-1}$, which is derived from the carbon density peaking ratio of Cp. Here the negative $R/L_{n,c}$ value represents the normalized carbon density gradient in the hollow profile and the positive value represents the normalized density gradient in the peaked profile. The ion thermal diffusivity is low ($\sim$ 1 m^2/s) when the carbon density profile inside ITB regime is peaked ($R/L_{n,c} > 0$), flat ($R/L_{n,c} = 0$), or slightly hollow ($-5 < R/L_{n,c} < 0$). However, the ion thermal diffusivity sharply increases when the carbon density profile inside ITB regime becomes significantly hollow ($R/L_{n,c} < -5$) and reaches > 10 m^2/s in the plasma with impurity hole, where the carbon density profile becomes extremely hollow. These results show that there is no significant difference in ion

thermal diffusivity between hydrogen plasma and deuterium plasma for the same impurity gradient. The critical value of normalized carbon density gradient $R/L_{n,c}$ for the enhancement of transport (increase of ion thermal diffusivity) is -5.

It is expected theoretically that the positive impurity gradient destabilizes the ITG turbulence[1, 2, 18–20]. After the formation of ITB, the ITG turbulence becomes unstable due to the increase of the ion temperature gradient because the density profile is flat. In the hydrogen plasma, the ITG turbulence is expected to be destabilized due to the formation of impurity hole (hollow impurity profile) and to cause the degradation of ion confinement. However, in the deuterium plasma, the ITG turbulence is expected to be stabilized due to the negative impurity density gradient. The stabilization of the ITG turbulence contributes to the sustainment of the steady-state ITB (no decrease of central ion temperature). This hypothesis is consistent with simultaneous decreases of carbon density ratio and central ion temperature in the hydrogen plasma plotted in figure 2 and the dependence of central ion temperature on carbon density peaking factors plotted in figure 3(a). The absolute value of this negative critical impurity density gradient is comparable to the level where the simulation predicts the enhancement of transport (increase of heat flux for given ion temperature gradient) [19]. In this simulation, the increase of heat flux for given ion temperature gradient is expected on both sides of impurity density gradient (both positive and negative $R/L_{n,c}$). Therefore it is interesting to study how the ion heat transport is affected when the impurity density profile is peaked and its gradient becomes significantly large. Although the slight increase of ion thermal diffusivity is observed at positive region (peaked carbon profile) above 5, the parameter region in this experiment is too narrow to discuss the existence of critical value of normalized carbon density gradient in the positive region.

In addition to ITG, there is another important instability, called TEM (trapped electron mode). Recently, isotope effects of trapped electron modes in the presence of impurities in tokamak plasmas have been reported[21]. The effects of impurities on the TEMs are substantially destabilizing when the density gradient of the impurity ions has the same sign as that of electrons as in $L_{ez} = L_{ne}/L_{nz} > 0$. In contrast, impurity ions have stabilizing effects on TEMs when the impurity ion density profile peaks opposite to that of the electrons, i.e. $L_{ez} < 0$. In this experiment, the electron density profiles are flat inside the ITB region. In the plasma with ion-ITB (high T_i/T_e plasma) plasma in LHD, the ITG is predicted to be unstable only in the core ($r_{\rm eff}/a_{99} < 0.5$) region while TEM is predicted to be unstable near the edge ($r_{\rm eff}/a_{99} > 0.8$)[22]. Therefore, this experiment is not suitable for testing the impact of impurity density gradient in TEM.

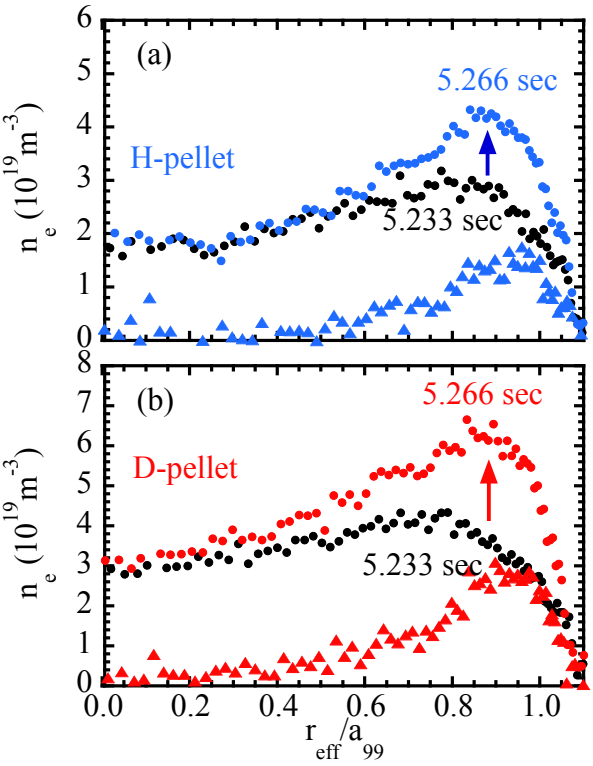

FIG. 5: Radial profile of electron density before (5.233 sec) and after (5.266 sec) the (a) hydrogen (#142326) and (b) deuterium (#142325) pellet injection. The radial proles of the increments of electron density due to pellet injection are also plotted.

III. ISOTOPE EFFECT ON BULK ION TRANSPORT

Hydrogen or deuterium pellet is injected into the D-H mixture plasma and hydrogen and deuterium density profiles are measured with charge exchange spectroscopy. The deposition of particles by pellet injection is estimated with the increment of electron density after the pellet injection by subtracting the electron density profile just before the pellet injection (t= 5.233 sec) from just after the pellet injection (t= 5.266 sec) as seen in figure 5. The density profile becomes hollow after the pellet injection and the deposition location of the pellet estimated from the peak position of the increment of the density is 4.5m in major radius ($r_{\rm eff}/a_{99} = 0.91$). Although the deposition of the pellet is near the plasma periphery, the core density increases after the pellet injection due to the inward convection of the particle fueled by the pellet. The deposition location of the pellet is essentially the same between H-pellet and D-pellet.

Bulk charge exchange spectroscopy system has been installed in LHD to measure the radial profiles of $n_H/(n_H+$

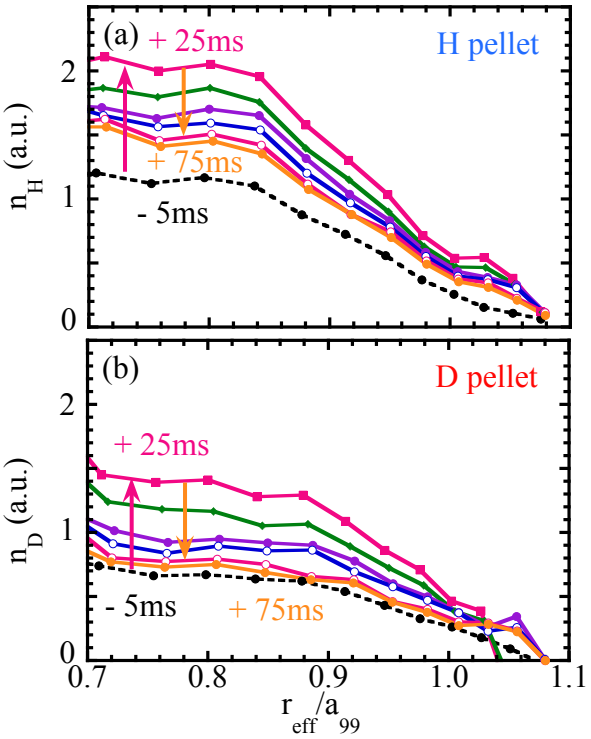

FIG. 6: Radial proles of (a) hydrogen density after the hydrogen pellet injection and (b) deuterium density after the deuterium pellet injection for the time slices Δt = -5, 25, 35, 45, 55, 65, 75, 85, and 95 ms. Here, Δt is the relative time with respect to the pellet injection.

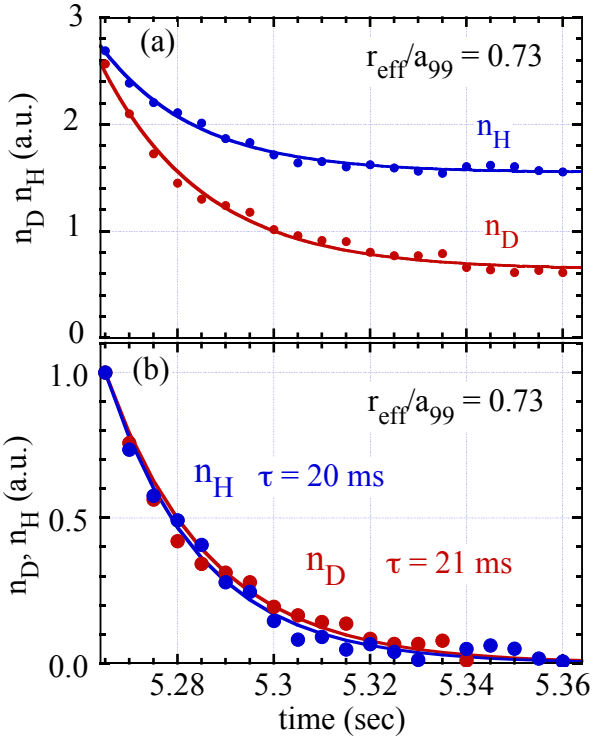

FIG. 7: (a) Decay of hydrogen density after the hydrogen pellet and deuterium density after the deuterium pellet injection at $r_{\rm eff}/a_{99} = 0.73$ for the recycling ratio of $\Gamma_H/\Gamma_D \sim 1.5$ and hydrogen beam fueling and (b) decay after subtracting the offset.

n_D) and $n_D/(n_H + n_D)$ in the plasma from H_α and D_α lines emitted by the charge exchange reaction between the bulk ions and the neutral beam injected[23–25]. In order to investigate the isotope effect on ion particle transport, the decay time of deuterium and hydrogen ions (not the electron density) is measured using Hα and Dα bulk charge exchange spectroscopy after the H pellet and D pellet injections. Figure 6 shows the time evolution of radial profiles of hydrogen density 5 ms before and after the hydrogen pellet and deuterium density 5ms before and after the deuterium pellet injection. Although ablation of the pellet is near the plasma periphery, significant increases of ion density of the pellet are observed 25 ms after the pellet injection. Hydrogen and deuterium density increase by 2.5 times due to the particle fueling of hydrogen and deuterium pellet, respectively. Then the ion density gradually decreases towards the level before the pellet injection. Hydrogen density decay is saturated at 85 ms because of the recycling, while the deuterium density keeps decreasing even 95 ms after the pellet injection. It should be noted that the hydrogen and deuterium density are almost unchanged after the D pellet and H pellet injection, respectively. The isotope mixing observed in TFTR or in JET [26, 27], where the different isotope species have the same radial profile regardless of the source, was not observed in this experiment. This is due to the difference in turbulence type between JET and LHD. ITG turbulence is dominant in JET plasma but it is not always dominant in LHD. After the formation of ITB, the bulk ion becomes peaked associated with the increase of hollowness of impurity with unchanged electron density profile in LHD[28]. The simultaneous peaking of bulk ion and hollowing of impurity ions with unchanged flat electron density profile imply that the electron particle transport is dominant in the plasma and ion species can have different profiles without the isotope mixing.

The difference in the ion particle transport between hydrogen and deuterium can be studied from the decay time of hydrogen density after H pellet and that of deuterium density after D pellet inside the deposition layer. Figure 7 shows the decay of hydrogen density after the hydrogen pellet and deuterium density after the deuterium pellet injection at $r_{\rm eff}/a_{99} = 0.73$. Both hydrogen and deuterium density show exponential decay with offset. The offset of hydrogen is twice that of hydrogen. In this experiment, the isotope wall recycling ratio $\Gamma_H/\Gamma_D \sim 1.5$ and beam isotope is hydrogen. Therefore, the higher offset level of hydrogen can be attributed to the hydrogen

beam-fueling and higher hydrogen recycling. The time evolution of hydrogen and deuterium density after subtracting their offset in figure 7(b) shows that the decay of hydrogen density is almost identical to that of deuterium. The decay time of hydrogen density is 20 ms and that of deuterium is 21 ms. In these discharges, there are no significant isotope differences in ion particle transport between hydrogen and deuterium ions.

IV. DISCUSSION AND SUMMARY

This paper reports important findings on the isotope effect on particle transport. Speed of impurity hole formation after the ITB is slower in deuterium plasma than in hydrogen plasma. The slowdown of the impurity hole formation speed postpones the time when the negative impurity gradient reaches the critical value of $R/L_{n,c} = -5$ and results in the longer sustainment of good confinement (lower ion thermal diffusivity near the magnetic axis). Therefore, the reduction of outward convection of impurity transport in deuterium plasma is primary isotope effect and the longer sustainment of ITB state in the deuterium plasma is considered to be a secondary isotope effect due to the mitigation of impurity hollow. The radial profile of hydrogen (H) and deuterium (D) ion density are measured from H_α and D_α lines emitted by the charge exchange reaction between the bulk ions and the neutral beam injected using the bulk charge exchange spectroscopy inside the isotope mixture plasma. The decay time of H ion density after the H-pellet injection and the decay time of D ion density after D-pellet injection are almost identical, which demonstrates that there is no significant isotope effect on ion particle transport.

V. ACKNOWLEDGMENTS

The authors are grateful to the technical staff of LHD for their excellent support for this work. One of the authors (KI) acknowledges Dr. M. Yoshida (National Institutes for Quantum and Radiological Science and Technology; QST) for providing us two spectrometers for the bulk charge exchange spectroscopy. This work is supported by the National Institute for Fusion Science grant administrative budgets (NIFS10ULHH021) and JSPS KAKENHI Grant Numbers JP15H02336, JP16H02442, JP17H01368

[1] Dong, J.Q., Horton, W., Dorland, W., *Phys. Plasmas* **1**, 3635 (1994).
[2] Dong, J.Q., Horton, W., *Phys. Plasmas* **2**, 3412 (1995).
[3] Ida, K., *et al. Rev. Rev. Lett.* **86** 5297 (1995).
[4] Ida, K., *et al. Phys. Plasmas* **16**, 056111 (2009).
[5] Morita, S., *et al. Plasma Sci. Technol.* **8** 55 (2006).
[6] Ida, K. and Fujita, T. *Plasma Phys. Control Fusion* **60**, 033001 (2018).
[7] Sakamoto, R., *et al. Nucl. Fusion* **41**381 (2001).
[8] Ida, K., *et al. Nucl. Fusion* **49**, 095024 (2009).
[9] Nagaoka, K., *et al. Nucl. Fusion* **55**, 113020 (2015).
[10] Osakabe, M., *Plasma Phys. Control Fusion* **56** 095011 (2014).
[11] Yoshinuma, M., *et al. Nucl. Fusion* **49** 062002 (2009).
[12] Yoshinuma, M., *et al. Nucl. Fusion* **55** 083017 (2015).
[13] Yoshinuma, M., *et al. Fusion Sci. Technol.* **58**, 375 (2010).
[14] Tanaka, K., *et al. Nucl. Fusion* **57**, 116005 (2017).
[15] Guo, W., *et al. Phys. Plasmas* **23**, 112301 (2016).
[16] Takahashi, H., *et al. Nucl. Fusion* **58**, 106028 (2018).
[17] Mukai, K., *et al. Plasma Phys. Control Fusion* **60** 074005 (2018).
[18] Kim, K., *et al. Phys. Plasmas* **24**, 062302 (2017).
[19] Bonanomi, N., *et al. Nucl. Fusion* **58**, 026028 (2018).
[20] Bonanomi, N., *et al. Nucl. Fusion* **58**, 036009 (2018).
[21] Yong Shen *et al. Plasma Phys. Control Fusion* **58** 045028 (2016).
[22] Nakata, M., *et al. Plasma Phys. Control Fusion* **61** 014016 (2019).
[23] Yamazaki, K., *et al. Plasma. Fusion. Res.* **13**, 1202103 (2018).
[24] Haskey, S.R., *et al. Rev. Sci. Instrum.* **89**, 10D110 (2018).
[25] Haskey, S.R., *et al.Plasma Phys. Control Fusion* **60** 105001 (2018).
[26] Efthimion, P.C., *et al. Rev. Rev. Lett.* **75** 85 (1995).
[27] Bourdelle1, C., *et al. Nucl. Fusion* **58**, 076028 (2018).
[28] Perek, A., *et al. Nucl. Fusion* **57**, 076040 (2017).